A&A 529, A123 (2011)
DOI: 10.1051/0004-6361/201116725

Astronomy & Astrophysics

Period persistence of long period oscillations in sunspots

N. Chorley[1], C. Foullon[1], B. Hnat[1], V. M. Nakariakov[1,2], and K. Shibasaki[3]

[1] Centre for Fusion, Space and Astrophysics, Physics Department, University of Warwick, Coventry CV4 7AL, UK
e-mail: n.d.y.chorley@warwick.ac.uk
[2] Central Astronomical Observatory of RAS at Pulkovo, 196140 St Petersburg, Russia
[3] Nobeyama Solar Radio Observatory/NAOJ, 384-1305 Nagano, Japan

Received 15 February 2011 / Accepted 24 March 2011

ABSTRACT

Long period oscillations in the microwave radiation intensity generated over the sunspot of NOAA AR 10330 are studied with the Nobeyama Radioheliograph as the sunspot passes over the solar disk, over the course of 9 days (06–15 April 2003). Periodogram, Fourier and global wavelet analyses reveal the presence of a significant oscillatory component in the range $P \approx 50$–120 min over the course of the observations. The spectral amplitudes of five significant Fourier components in the range $P = 50$–150 min are also seen to be stable over the observations, when the data are not affected by changes in magnetic configuration in the region. The ground-based nature of the instrument naturally introduces long data gaps in such long duration observations and the presence of the gaps does not allow any conclusion as to the stability of the phases of the oscillations. As a model to explain the persistence of the dominant long periods, a simple oscillator with a nonlinear driving term is proposed. The spectral difference between distinct peaks within, e.g. the 3 min spectral band, is expected to be able to resonate with the long period one hour oscillations.

Key words. Sun: oscillations – Sun: activity – sunspots

1. Introduction

Sunspots are the most visible manifestation of the solar magnetic field in lower regions of the solar atmosphere and are interesting features to study as they may provide clues about the nature of the mechanism for generating the magnetic field, the solar dynamo. Associated with them may be filaments – dark, cool structures which lie parallel to the magnetic polarity inversion line in the region.

Long period ($P > 10$ min) oscillations in sunspots could be connected with large scale reconfiguration of the Sun's magnetic field, or even the leakage of waves (g-modes) from the solar interior. The nature of such oscillations is not understood, though several studies have sought to answer this question. Berton & Rayrole (1985), using photospheric magnetic and velocity data in the neutral iron line $\lambda = 630.2$ nm, first observed torsional oscillations in the umbral magnetic field of a sunspot, with periods of approximately 45 min and suggested that these could be related to magnetohydrodynamic (MHD) oscillations generated at the top of the solar convection zone. Sunspot penumbrae were also found to oscillate, as reported by Druzhinin et al. (1993), in the Doppler velocity of two spectral lines of photospheric origin (with periods around 60 min). Moreover, optical observations by Nagovitsyna & Nagovitsyn (2002) indicated two kinds of oscillation mode, with periods ranging from 40 to 100 min – one associated with sunspots and the other with pores (sunspots without umbrae). Nagovitsyna & Nagovitsyn (2001) also used optical observations to detect quasi-hourly oscillations in magnetic fragments in sunspots, finding that the oscillation had its maximum amplitude in the penumbra and that there was an anisotropy of the oscillation in the azimuthal direction.

More recently, Efremov et al. (2009) detected periods of 60–80 min in the Doppler shift of six spectral lines formed at different heights in the sunspot atmosphere and found that the power of the long periods decreases with height; the oscillations were well pronounced at a height of 200 km and barely seen at a height of 500 km. Efremov et al. (2010) detected periods in the range 40–180 min in wavelengths formed between 190 km and 535 km (periods of 250 and 480 min were found in the line-of-sight magnetograms from space-borne SOHO/MDI data).

In microwave emission above sunspots, oscillations of tens and hundreds of minutes have been detected (Gelfreikh et al. 2006; Chorley et al. 2010) with the Nobeyama Radioheliograph (NoRH, Nakajima et al. 1994). In particular, Chorley et al. (2010) indicated the presence of two periodicities in each analysed sunspot. Spatial analysis revealed that most of the spectral power was located above the umbral regions and strongly suggested that there were two regions of coherent oscillation that oscillated in anti-phase with each other.

Finally, it may be noted that long period oscillations have also been observed in coronal structures, which all have the source of their magnetic fields in sunspots. For example, Foullon et al. (2004, 2009) detected periods of several hours in extreme ultraviolet (EUV) observations of solar filaments (using SOHO/EIT) and Verwichte et al. (2010) studied transverse oscillations in large coronal loops observed with TRACE and SOHO/EIT, with periods between 24 and 180 min.

In this paper, we study 9 successive observation intervals of one of the sunspots studied by Chorley et al. (2010) in order to investigate the lifetime of the long period oscillations. The paper is organised in the following way: Sect. 2 presents the observations and preprocessing of the data and in Sect. 3, we detail our analysis and results. Finally, in Sect. 4, we discuss our results and propose a simple model for the generation of the observed oscillations.

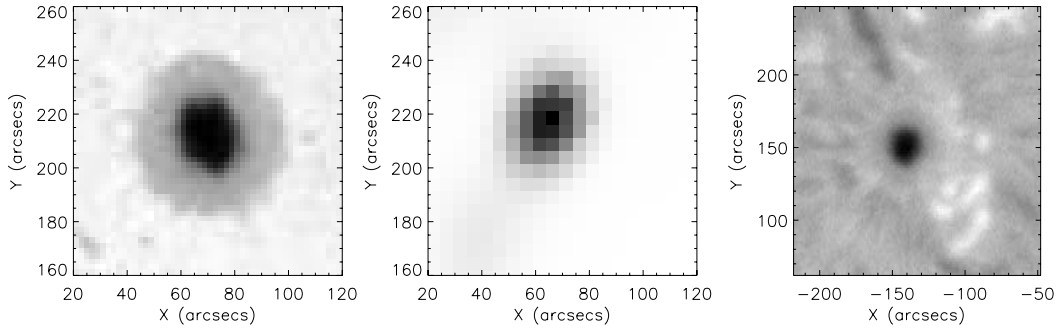

Fig. 1. Images of AR 10330 in white light (*left*) and microwave (17 GHz, *centre*) taken at 23:59 UT on 09 April 2003 and in Hα (*right*), taken at 01:03 UT on 10 April 2003.

2. Observations

The sunspot of NOAA active region (AR) 10 330 was observed over intervals of approximately 7.25 h on 9 successive days with NoRH (based in Japan), beginning on 06 April 2003 and ending on 15 April 2003. The observations began at 22:45 UT on each day and ended at around 06:30 UT the following day. At the beginning of the observation period, the region was located at a position of $(-572, 199)''$, relative to disk centre. For convenience, throughout this paper, we refer to observations on each date (e.g. time series) by a number corresponding to their position in the sequence of 9 days (i.e. 1 for 06 April, 2 for 07 April, etc.).

Figure 1 shows the region in white light (from SOHO/MDI) and microwave on 09 April 2003 and Hα (from the Yunnan Astronomical Observatory) on 10 April 2003. The Hα image shows evidence of a filament associated with the region, located north-west of the main region. This region has been studied by Sainz Dalda & Martínez Pillet (2005) and Zhang et al. (2007), who investigated moving magnetic features and their relation to penumbral filaments and evolution of the parent sunspot. The studies of both groups used data in the interval 09 April 2003 14:00 UT−10 April 2003 00:50 UT. In addition, the observations used in this work include those used in Chorley et al. (2010) (08 April 2003 22:45 UT−09 April 2003 06:30 UT).

Sequences of images were obtained for each date from NoRH at a frequency of 17 GHz. The emission is generated by the gyroresonant mechanism, where a low harmonic of the cyclotron frequency is equal to the frequency of the instrument (Shibasaki et al. 1994; Vourlidas et al. 2006). The images are of size 8×8 pixels, with a spatial resolution of $10''$ per pixel and the time cadence is 10 s. This is a restricted field of view to minimise the contribution from the quiet Sun. Due to the long intervals of observation, the solar rotation has to be taken into account. The starting position is converted to heliographic longitude and latitude and the change in longitude is found every 10 s. In this way, we obtain new centre coordinates for the next image from the coordinates of the previous one.

From each daily set of images, we generated a time series by computing the mean brightness temperature, T_B, of each image. Present in each time series is a large scale trend mainly due to the change in effective area of the instrument as the Sun passes overhead during the course of the local day. The trend is removed by fitting a 4th order polynomial and spectrally filtering the time series to remove oscillations with 3 cycles or fewer ($P \geq 145$ min). Figure 2 shows the resulting detrended time series.

Most of the time series generated in this way contain large increases in T_B, that are most likely to be flares, and several glitches. All such features are identified and then removed from the time series by interpolation with a cubic spline. To identify the flares, we set a threshold on T_B of 8.5×10^4 K for most time series (except for days 5 and 9, for which values of 6.5×10^4 K were used). For the amplitude study described in Sect. 3 below, we did not remove the spikes in the signals.

3. Analysis

We computed Fourier power spectra, Lomb-Scargle periodograms (Scargle 1982) and global wavelet spectra (see, e.g. Torrence & Compo 1998) for each detrended and interpolated time series in order to investigate the long period oscillations. Figure 3 shows the spectra obtained by each of these methods, for each of the 9 time series. It can be seen that long period oscillations in the range $P = 50-120$ min are present in all time series and that there are, in general, two long period peaks in the spectra.

Figure 4 presents information related to the solar activity and an analysis of the dominant periods, in order to determine whether any events in the region could have been responsible for changes in the observed period.

We obtained the full disk flux observed by the GOES spacecraft and identified flares and CMEs that occurred in AR 10330, as well as in other regions, during our observation period. This is shown in panel (a) and it is clear that the Sun was quite active during the entire 9 days of observations, as evidenced by the large number of peaks in the GOES flux. However, it can also be seen that there were two events in the region during the observations: a filament disappearance (beginning after 08 April 2003 00:45 UT and ending before 08 April 2003 13:02 UT) and a C class flare that occurred on 13 April 2003 at 08:45 UT. These events are indicated by dashed vertical lines.

In panel (b), we show the original time series generated from the sets of NoRH images. Large increases in brightness temperature can be seen, which do not appear to coincide with peaks in the GOES flux. The reason for this could be that small events (relative to the full disk flux) in the region do not necessarily appear in the full disk GOES flux, but can cause large local brightenings due to the restricted field of view. It can also be seen that there is a trend in the mean intensities in the signals over the 9 days of observations. For the first 7 of those days, the trend is roughly symmetric about the interval between signals 3 and 4, when the sunspot crosses the central meridian. In addition, the mean intensity is seen to decrease for signals 8 and 9, which is attributed to the sunspot being positioned close to the limb on those days and both of these points are suggestive of a projection effect.

In panel (c), we show the dominant periods (i.e. the periods corresponding to the highest spectral peak) in the range

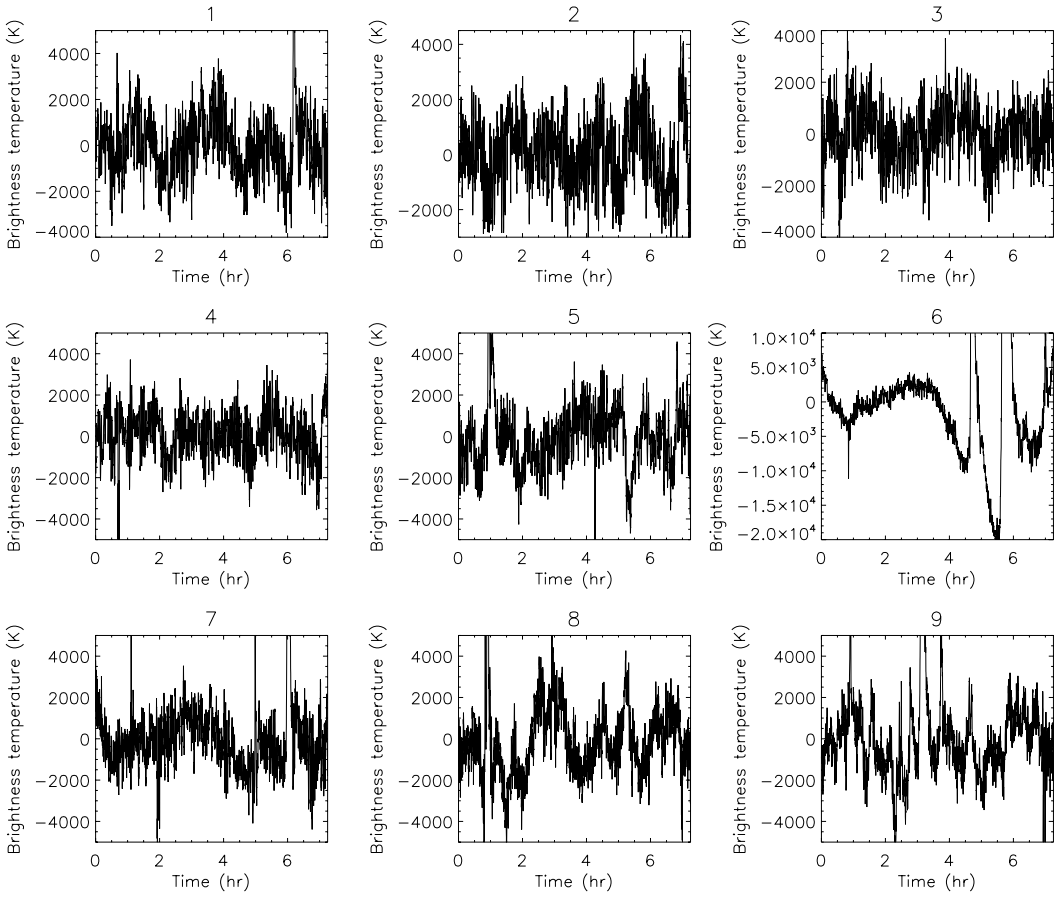

Fig. 2. Time series of microwave intensity generated from sequences of images of AR 10330 obtained with NoRH. The signals have been detrended with a 4th order polynomial. The title for each signal gives the day number in the sequence of the 9 days of observation.

P = 50−120 min and all three methods give similar values (within the error bars of the global wavelet), except in the last case. It can also be seen that the dominant period remains quite stable over the course of the observations. The dominant period appears to reach a local minimum in signal 7 before the flare in the region and is seen to rise after it. This decrease in period could be associated with changes in magnetic configuration that may or may not lead to a flare.

In panel (d), the power of each of the 5 long period Fourier components in the range P = 50−150 min is shown for each of the 9 days. The signals were first filtered to contain only periods in this range, using a boxcar function as the filter. The first feature of note is the large rise in power in all 5 components for signal 6. This is artificial since the time series contains large peaks (see Fig. 2) that are of a finite width and as such, the detrending procedure introduces an artificial oscillation whose period is close to those of interest. The amplitudes for all components over the days excluding day 6 do not appear to vary by a large amount.

We also attempted to investigate the change in phase of the long period oscillations over the 9 days of observations in the following way. For each of the 5 Fourier components in the range P = 50−150 min range (after filtering), we found the phase for each of the 9 signals. Naturally, one is interested in the phase of the oscillation at some common reference point, here chosen as the beginning of the observations (06 April 2003 22:45 UT). In order to obtain Fourier phases with respect to this common reference, we made use of the time delay relation of the Fourier transform $\mathcal{F}$, of a signal $I(t)$,

$$\mathcal{F}[I(t-t_0)] = \mathcal{F}[I(t)]\,\mathrm{e}^{-\mathrm{i}2\pi f t_0}, \quad (1)$$

where t_0 is the time delay and f the frequency. Equation (1) tells us that a time delay is seen as a phase shift in the Fourier transform. In order to obtain the phase of the oscillation at the beginning of the observations, we divide $\mathcal{F}[I(t-t_0)]$ by $\mathrm{e}^{-\mathrm{i}2\pi f t_0}$ to give $\mathcal{F}[I(t)]$ and then find the phase from the real and imaginary parts of the relevant component. Figure 5 shows a polar plot of the phases for each of the 5 components, on each of the 9 days. It is clear that the phases for different components behave in different ways over time and that there does not seem to be any long term stability in the phases (over the entire course of the observations).

4. Discussion and conclusions

We have analysed nine 7.25 h intervals of microwave emission at 17 GHz over NOAA AR 10330, observed with the Nobeyama Radioheliograph. The main finding of this study is that long period oscillations ($P \geq 50$ min) are found to be present in each of the analysed time intervals and the dominant long period component appears to be stable over the observations. The apparent change in period between 13 April 2003 06:30 and 13 April 2003 22:45 (the interval between signals 7 and 8) could be due to changes in magnetic configuration in the region. In addition,

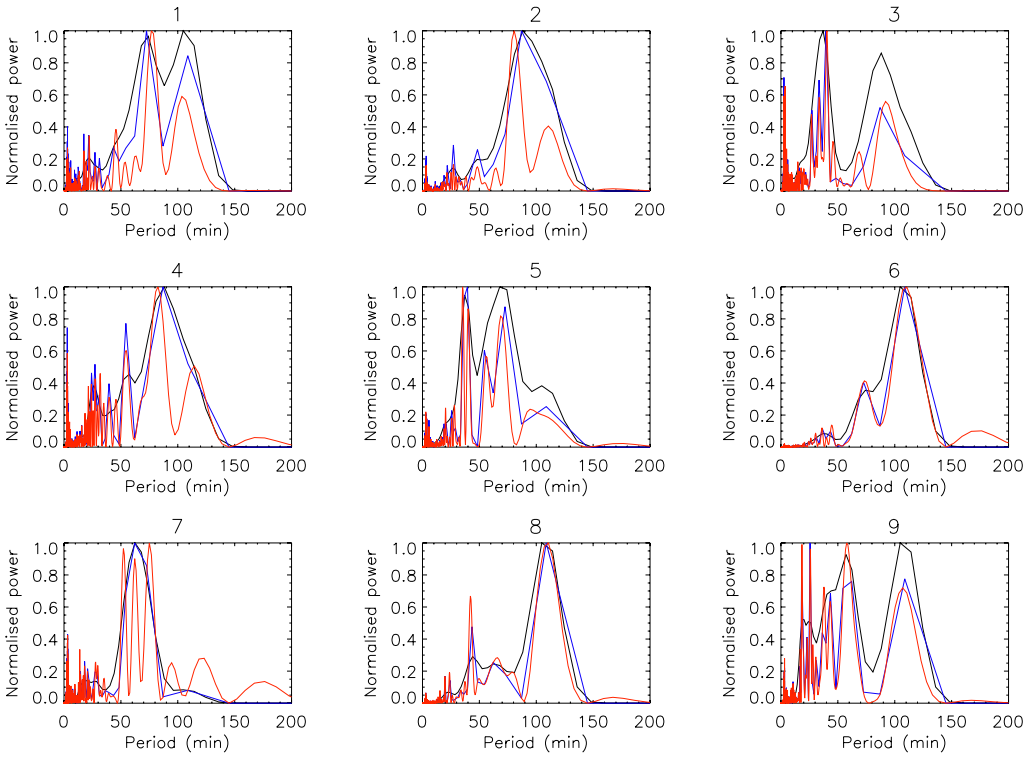

Fig. 3. Normalised power spectra obtained for each of the 9 detrended signals, using the global wavelet (black), Lomb-Scargle periodogram (red) and FFT (blue). Each spectrum has been normalised to its maximum amplitude. As in Fig. 2, the title for each signal gives its position in the sequence of the 9 days of observation.

the spectral amplitude of 5 Fourier components in the range $P = 50-150$ min shows stability over the course of the observations, when the data are not influenced by changes in magnetic configuration or large flares (as on day 6). The large time gaps between the data sets, together with the noise in the signals do not allow us to draw any firm conclusions about the stability of the phases of the oscillations.

Long period oscillations in sunspots can be associated, for example, with the global oscillations of the sunspots in terms of the shallow sunspot model (Solov'ev & Kirichek 2008). However, the persistence of those oscillations requires the answer to an additional question: what is the physical mechanism that excites those modes in the quiet Sun and how are the oscillations maintained against the damping? One possibility is the resonance between a certain driver and the natural frequency of the sunspot. Such a driver could be associated with the 3 min oscillations of sunspots, which are known to be very persistent narrowband features. Usually, 3 min oscillations are seen to have a fine spectral structure, having multiple peaks (see, e.g. Shibasaki 2001; Gelfreikh et al. 1999). The average spectral width of the cluster of 3 min peaks corresponds to a period of about an hour and hence, it can resonate with the long period oscillations of a sunspot, exciting the long period oscillations and compensating for the damping. However, such a process is possible only in the presence of nonlinear effects.

To illustrate this possibility, we consider a driven simple harmonic oscillator in which the driver is nonlinear, e.g.

$$\frac{\mathrm{d}^2 I}{\mathrm{d}t^2} + k\frac{\mathrm{d}I}{\mathrm{d}t} + \omega_0^2 I = \left[\sum_{i=1}^{m} A_i \cos(\omega_i t + \phi_i)\right]^2, \qquad (2)$$

where k is the damping coefficient, ω_0 is the natural frequency of oscillation (corresponding to a period of $P \approx 100$ min), the A_i, ω_i and ϕ_i are the amplitudes, frequencies and phases of the driving oscillations and m is the number of driving oscillations, which represent individual peaks of 3 min oscillations. The nonlinearity represents some physical mechanism responsible for the coupling of 3 min and long period oscillations. For example, it can be the modification of characteristic speeds of long period oscillations by the 3 min oscillations.

We stress that Eq. (2) is an empirical model that reflects the observed properties of the oscillations. As such, we make no attempt to estimate the value of k, but only include damping in the model as we know it is a physical effect (due to, e.g. viscosity or leakage of the oscillations to the corona). In addition, ω_0 is related to the magnetic field strength, sunspot depth and mass density as given in Solov'ev & Kirichek (2008).

Expanding the expression on the right hand side of Eq. (2) leads to two kinds of terms, for $i \neq j$:

(i) $\cos^2 \omega_i t$, which can be expressed in terms of $\cos 2\omega_i t$;
(ii) $\cos \omega_i t \cos \omega_j t$, which can be expressed in terms of $\cos\left(\omega_i + \omega_j\right) t$ and $\cos\left(\omega_i - \omega_j\right) t$.

The first kind of term gives frequency doubling and we suggest that a broadband spectrum of solar 5 min oscillations can contribute to the 3 min oscillations. The second kind of term, in particular the $\omega_i - \omega_j$ kind, suggests that two frequencies close together will generate a low frequency oscillation. As explained above, we suggest that the 3 min part of the spectrum is responsible for this effect.

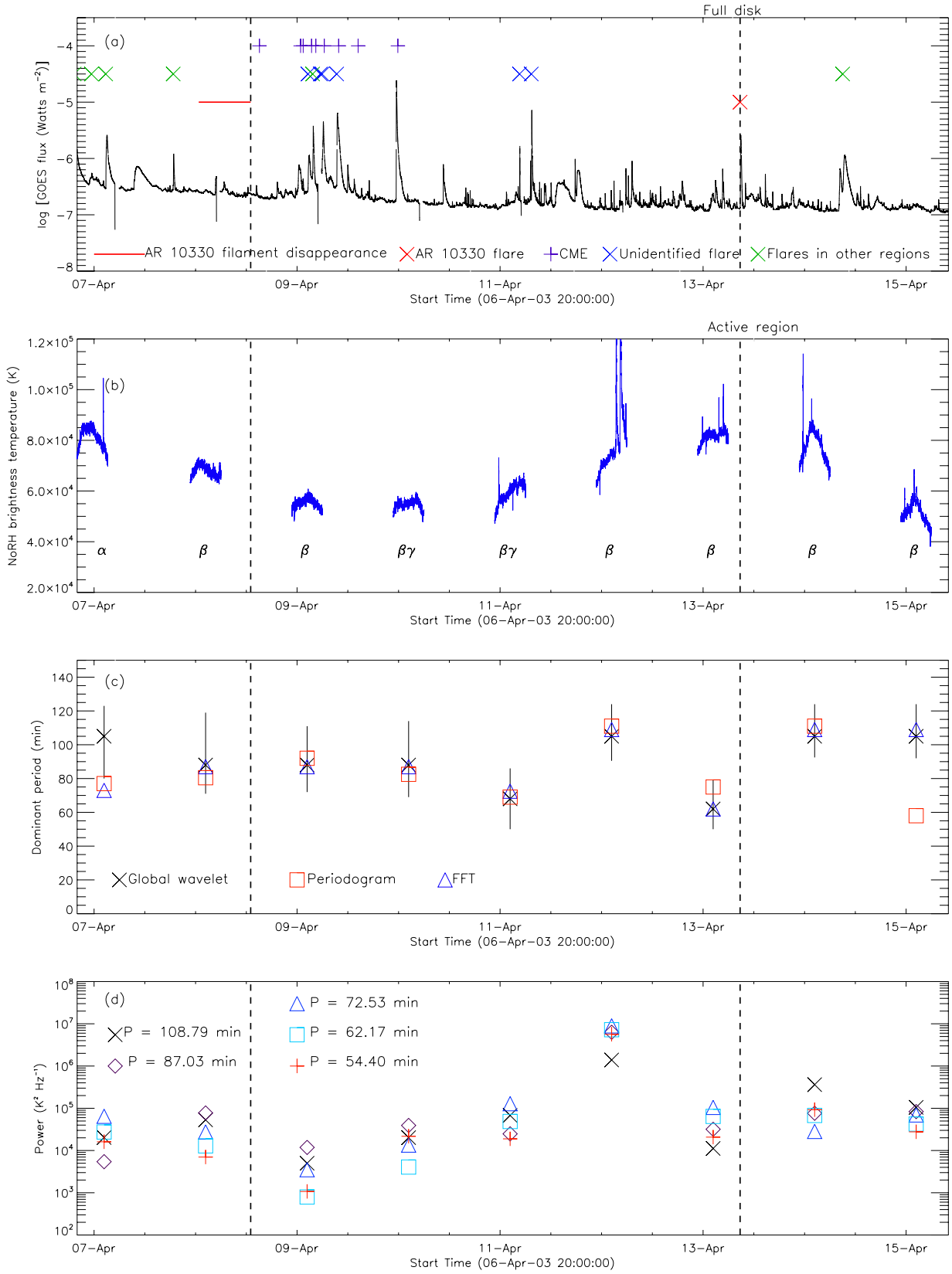

Fig. 4. a) The GOES X-ray flux during the period 06 April 2003 20:00–15 April 2003 10:00, showing events that occurred in AR 10330 and elsewhere. **b)** The original time series obtained from NoRH images. The Mt. Wilson classification for AR 10330 is also shown. **c)** The dominant periods in the range P = 50–120 min, obtained with all three of the methods for computing the power spectrum. The error bars on the global wavelet spectrum were obtained using the full width at half maximum (FWHM) of the corresponding spectral peak. **d)** The power for each Fourier component in the range P = 50–150 min for each day. In panels **c)** and **d)**, the points for each day have been plotted at the midpoint of each signal.

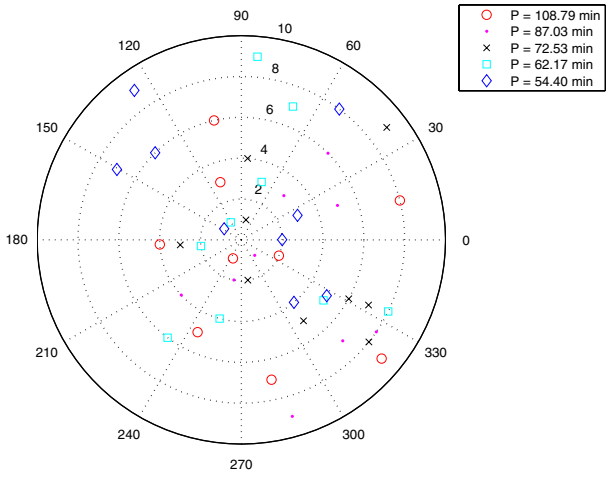

Fig. 5. The phases for each Fourier component over the 9 days of observation after filtering the signals to contain only periods in the range $P = 50-150$ min. Phases are given in degrees and the points for each day lie on an annulus at $r = 1, 2, \ldots, 9$, corresponding to the day number (i.e. 1 for 06 April 2003, 2 for 07 April, etc.).

The results presented in this paper demonstrate the need for the long-term study of long period oscillations in sunspots, their possible relationship with 3 min oscillations and theoretical modelling of these oscillations.

Acknowledgements. N.C. is supported by an EPSRC studentship. C.F. acknowledges financial support from the UK Science and Technology Facilities Council (STFC) on the CFSA Rolling Grant. The Nobeyama Radioheliograph is operated by the Nobeyama Solar Radio Observatory (NAOJ).

References

Berton, R., & Rayrole, J. 1985, A&A, 152, 219
Chorley, N., Hnat, B., Nakariakov, V. M., Inglis, A. R., & Bakunina, I. A. 2010, A&A, 513, A27
Druzhinin, S. A., Pevtsov, A. A., Levkovsky, V. L., & Nikonova, M. V. 1993, A&A, 277, 242
Efremov, V. I., Parfinenko, L. D., & Solov'ev, A. A. 2009, Cosm. Res., 47, 279
Efremov, V. I., Parfinenko, L. D., & Solov'ev, A. A. 2010, Sol. Phys., 267, 279
Foullon, C., Verwichte, E., & Nakariakov, V. M. 2004, A&A, 427, L5
Foullon, C., Verwichte, E., & Nakariakov, V. M. 2009, ApJ, 700, 1658
Gelfreikh, G. B., Grechnev, V., Kosugi, T., & Shibasaki, K. 1999, Sol. Phys., 185, 177
Gelfreikh, G. B., Nagovitsyn, Y. A., & Nagovitsyna, E. Y. 2006, PASJ, 58, 29
Nagovitsyna, E. Y., & Nagovitsyn, Y. A. 2001, Ast. Lett., 27, 118
Nagovitsyna, E. Y., & Nagovitsyn, Y. A. 2002, Ast. Lett., 28, 121
Nakajima, H., Nishio, M., Enome, S., et al. 1994, IEEE Proc., 82, 705
Sainz Dalda, A., & Martínez Pillet, V. 2005, ApJ, 632, 1176
Scargle, J. D. 1982, ApJ, 263, 835
Shibasaki, K. 2001, ApJ, 550, 1113
Shibasaki, K., Enome, S., Nakajima, H., et al. 1994, PASJ, 46, L17
Solov'ev, A. A., & Kirichek, E. A. 2008, Astrophys. Bull., 63, 169
Torrence, C., & Compo, G. P. 1998, Bull. Am. Meteorol. Soc., 79, 61
Verwichte, E., Foullon, C., & Van Doorsselaere, T. 2010, ApJ, 717, 458
Vourlidas, A., Gray, D. E., & Shibasaki, K. 2006, PASJ, 58, 11
Zhang, J., Solanki, S. K., Woch, J., & Wang, J. 2007, A&A, 471, 1035